

Metastable superconducting state in quenched $K_xFe_{2-y}Se_2$

Fei Han^a, Huan Yang^b, Bing Shen^a, Zheng-Yu Wang^a, Chun-Hong Li^a and Hai-Hu Wen^{b*}

^a*National Laboratory for Superconductivity, Institute of Physics and Beijing National Laboratory for Condensed Matter Physics, Chinese Academy of Sciences, Beijing 100190, China;* ^b*Center for Superconducting Physics and Materials, National Laboratory of Solid State Microstructures and Department of Physics, Nanjing University, Nanjing 210093, China*

(v4.5 released May 2010)

By direct quenching or post-annealing followed by quenching, we have successfully obtained a series of $K_xFe_{2-y}Se_2$ samples with different properties. It is found that the samples directly quenched in the cooling process of growth show superconductivity and the one cooled with furnace is insulating even though their stoichiometries are similar. The sample cooled with furnace can be tuned from insulating to superconducting by post-annealing and then quenching. Based on the two points mentioned above, we conclude that the superconducting state in $K_xFe_{2-y}Se_2$ is metastable, and quenching is the key point to achieve the superconducting state. The similar stoichiometries of all the non-superconducting and superconducting samples indicate that the iron valence doesn't play a decisive role in determining whether a $K_xFe_{2-y}Se_2$ sample is superconducting. Combining with the result got in the $K_xFe_{2-y}Se_2$ thin films prepared by molecular beam epitaxy (MBE), we argue that our superconducting sample partly corresponds to the phase without iron vacancies as evidenced by scanning tunneling microscopy (STM) and the insulating sample mainly corresponds to the phase with the $\sqrt{5} \times \sqrt{5}$ vacancy order. Quenching may play a role of freezing the phase without iron vacancies.

Keywords: $K_xFe_{2-y}Se_2$; direct quenching; post-annealing and then quenching; insulating; superconducting; metastable; iron vacancies

1. Introduction

Since the discovery of superconductivity at 26 K in oxy-pnictide $LaFeAsO_{1-x}F_x$ [1], enormous interests have been stimulated in the fields of condensed matter physics and material sciences. Among the several types of iron based superconductors with different structures[1–8], FeSe with the PbO structure has received special attention since its structure is simpler than other iron pnictide superconductors. However, the superconducting transition temperature (T_c) in iron chalcogenide compounds is not enhanced as high as other iron pnictide superconductors under ambient pressure until the superconductivity at above 30 K in $K_xFe_{2-y}Se_2$ is discovered[9]. The insulating and the superconducting state are both observed in $K_xFe_{2-y}Se_2$ with different stoichiometries and some groups have tuned the system from insulating to superconducting by varying the ratio of starting materials[10–12]. Here we give two new tuning methods: direct quenching or post-annealing followed by quenching. On one hand, by directly quenching at different furnace temperatures in the cooling process of growth we can get a series of $K_xFe_{2-y}Se_2$ samples with different superconducting properties, while the sample cooled with furnace slowly is non-

*Corresponding author. Email: hhwen@nju.edu.cn

superconducting but insulating. On the other hand, by post-annealing and then quenching we can tune the previous insulating $K_xFe_{2-y}Se_2$ sample into superconducting state again, which was discovered by us for the first time and confirmed by another group[15]. We also find that the tuning is reversible, since the superconducting state disappears about 20 days later and the insulating state comes out again in the post-annealed and quenched crystals. As mentioned above, we think that the quenching is important to the appearance of superconductivity and the superconducting state which needs to be frozen by quenching is metastable.

2. Sample preparation

By using the self-flux method, we successfully grown high-quality single-crystalline samples of $K_xFe_{2-y}Se_2$. First FeSe powders were obtained by the chemical reaction method with Fe powders (purity 99.99%) and Se powders(purity 99.99%). Then the starting materials in the fixed ratio of K: FeSe = 0.8: 2 were placed in an alumina crucible and sealed in a quartz tube under vacuum. All the weighing, mixing, grinding and pressing procedures were finished in a glove box under argon atmosphere with the moisture and oxygen below 0.1 PPM. The contents were then heated up to 1030 °C for 3 hours. Subsequently the furnace was cooled down to 750 °C at a rate of 5 °C/h. Below 750 °C, the sample cooled with furnace was kept in furnace and cooled down slowly to room temperature while the directly quenched samples were took out from furnace and quenched in air at different furnace temperatures. We cleaved some crystals from the previous sample cooled with furnace in the glove box, put them in a one-end-sealed quartz tube, and sealed the other end of the quartz tube with a closed valve. The valve was then connected with pump and opened under vacuum. To protect the crystals from heat, the quartz tube was wrapt with wet paper. All these made the quartz tube sealing procedure be performed with the crystals not exposed to air and not heated. After tube sealing, a post-annealing procedure is carried out on the crystals (enclosed in the evacuated quartz tube) with a heating plate at different temperatures for 1 hour and then the crystals were rapidly removed from the heating stage.

3. Experimental data and discussion

The X-ray diffraction (XRD) measurements of our samples were carried out on a *Mac – Science* MXP18A-HF equipment with a scanning range of 10° to 80° and a step of 0.01°. The DC magnetization measurements were done with a superconducting quantum interference device (Quantum Design, SQUID, MPMS-7T). The resistance data were collected using a four-probe technique on the Quantum Design instrument physical property measurement system (Quantum Design, PPMS-9T) with magnetic fields up to 9 T. The electric contacts were made using silver paste at room temperature. The data acquisition was done using a DC mode of the PPMS, which measures the voltage under an alternative DC current and the sample resistivity is obtained by averaging these signals at each temperature. In this way the contacting thermal power is naturally removed. The temperature stabilization was better than 0.1% and the resolution of the voltmeter was better than 10 nV.

3.1. Direct quenching

In Fig.1 we show the temperate dependence of dc magnetization for the sample cooled with furnace and the samples directly quenched at about 200 °C, 300 °C,

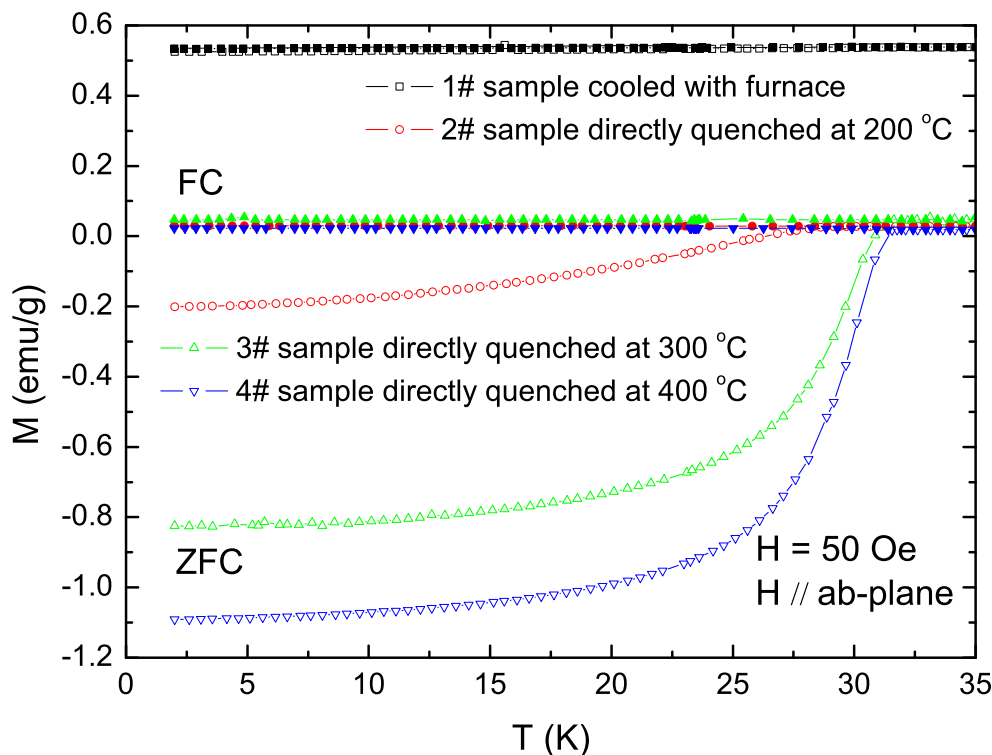


Figure 1. (Color online) Temperature dependence of dc magnetization for the sample cooled with furnace and the samples directly quenched at about 200 °C, 300 °C, and 400 °C, respectively. The measurements were carried out under a magnetic field of 50 Oe in zero-field cooled (ZFC) and field-cooled (FC) processes with the field parallel to the ab-plane.

and 400 °C, respectively. The measurements were carried out under a magnetic field of 50 Oe in zero-field cooled (ZFC) and field-cooled (FC) processes with the field parallel to the ab-plane. Paramagnetic signal is observed in the sample cooled with furnace and there is not diamagnetization in the low temperature regime. A weak diamagnetic signal, which is corresponding to superconductivity, appears below about 28 K in the sample directly quenched at 200 °C. When the quenching temperature increases to above 300 °C, strong diamagnetic signals appear below about 31.5 K. We find that the quenching temperature has an important influence on the diamagnetization signal. In sharp contrast to it, we find that the transition temperature does not strongly depend on the quenching temperature since the diamagnetization signals all appear below 28-32 K in the samples directly quenched at 200 °C, 300 °C, and 400 °C.

By electrical resistivity measurements we find that the non-superconducting sample cooled with furnace has a insulating behavior, as shown in in the top panel of Fig.2. The sample directly quenched at 200 °C has a superconducting transition at 32.5 K and a hump-like anomaly at 150 K in the curve of $\rho(T)$. The sample directly quenched at 300 °C and 400 °C is also superconducting with the same T_c as the sample directly quenched at 200 °C and the hump-like anomaly shifts to about 250 K. We find that the absolute value of resistivity decreases with the quenching temperature increasing from 200 to 400 °C, which is a strong support to that $K_x\text{Fe}_{2-y}\text{Se}_2$ is a phase-separation system composed of a metallic phase and a insulating phase.

We perform magnetization and resistivity measurements for several times and find both the magnetization and the resistivity results are reproducible, which indicates that the insulating property in the sample cooled with furnace and the superconductivity in the directly quenched samples is bulk.

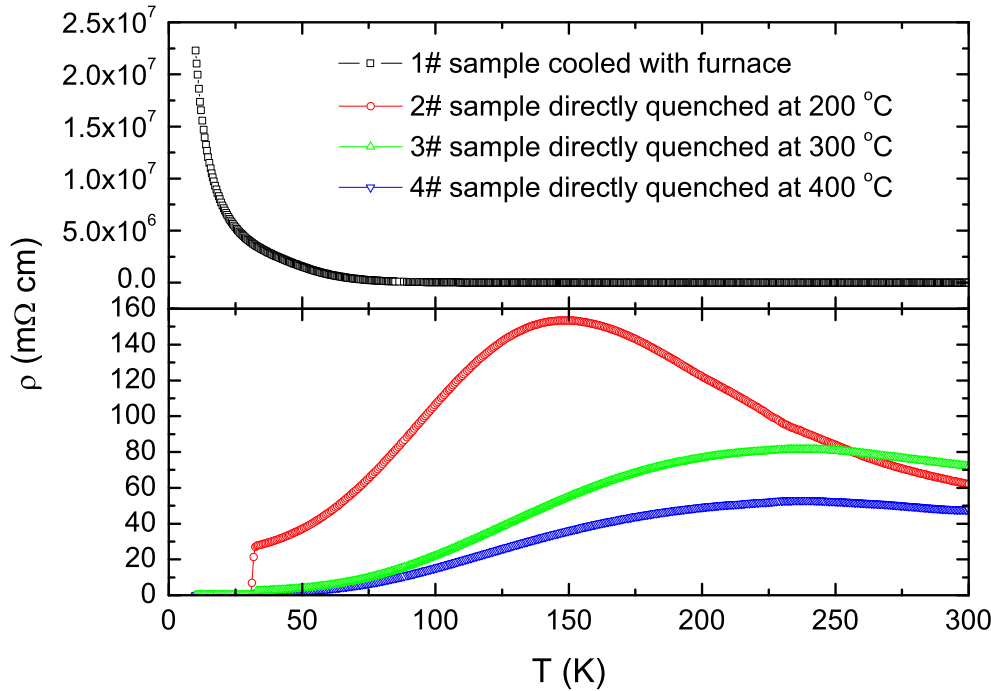


Figure 2. (Color online) Temperature dependence of resistivity for the sample cooled with furnace and the samples directly quenched at about 200 °C, 300 °C, and 400 °C, respectively.

To investigate what effect the quenching procedure has on the $K_xFe_{2-y}Se_2$ samples and why the superconductivity appears, we carried out X-ray diffractions on these samples and used inductively coupled plasma (ICP) to determine the stoichiometries of $K_xFe_{2-y}Se_2$ samples.

As shown in Fig.3, the peaks from the (00 l) reflections are still very sharp, indicating excellent crystalline quality. And we hardly find very obvious shifting among these peaks. However, the peaks marked by the asterisks in the samples directly quenched seem to shift closer to the nearby (008) and (00 $\bar{1}0$) peaks than in the sample cooled with furnace, which possibly indicates the two weak peaks come from a super-lattice of iron vacancies order and the phase with iron vacancies order peters out after quenching.

Table 1. Stoichiometries and iron valences for the sample cooled with furnace and the samples directly quenched at different temperatures while the nominal stoichiometries of these samples are fixed as $K_{0.8}Fe_2Se_2$.

Quenching temperature	Stoichiometry	Valence of iron
Cooled with furnace	$K_{0.80}Fe_{1.69}Se_2$	1.890
200 °C	$K_{0.76}Fe_{1.71}Se_2$	1.895
300 °C	$K_{0.78}Fe_{1.70}Se_2$	1.894
400 °C	$K_{0.76}Fe_{1.70}Se_2$	1.906

We find that the actual compositions and the iron valences of all the four samples are very similar to each other. It is noteworthy that the iron valences are all located at the non-superconducting region in the electronic and magnetic phase diagram of $K_xFe_{2-y}Se_2$ as a function of iron valence[12]. Based on this point, we think that the phase diagram as a function of iron valence didn't solve the problem what determines $K_xFe_{2-y}Se_2$ to be superconducting or not. There must be a more essential factor working effect instead of iron valence. We notice that different groups including our group got different results even though they prepared samples in a same

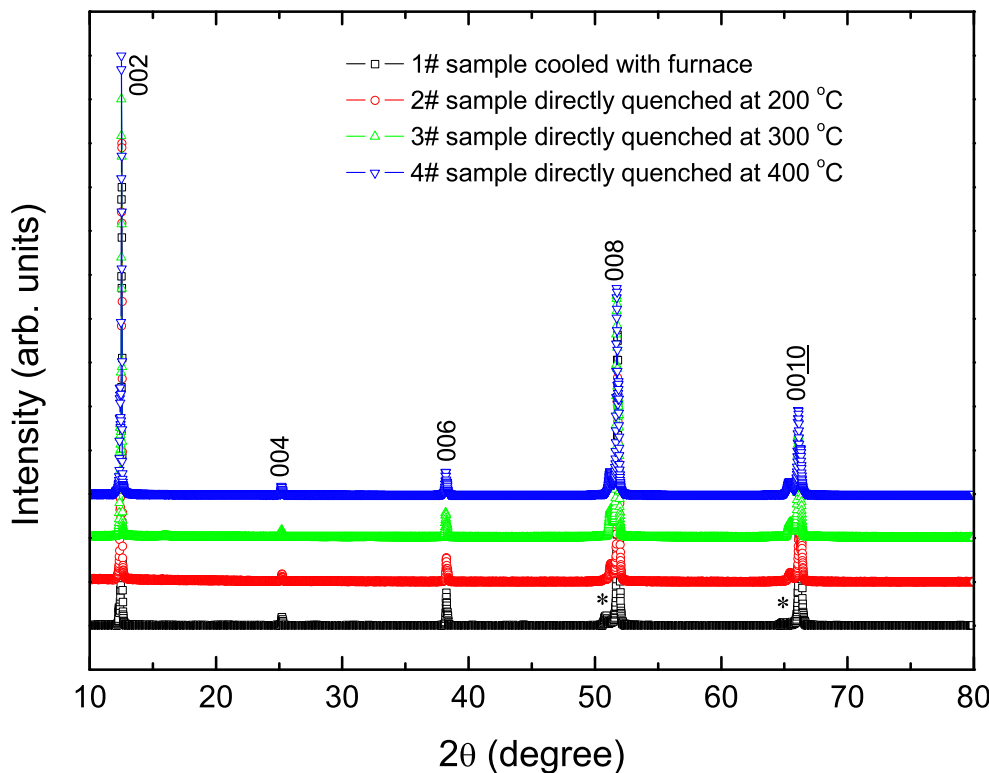


Figure 3. (Color online) X-ray diffraction patterns showing the (00 l) reflections from the basal plane of the $K_xFe_{2-y}Se_2$ sample cooled with furnace and the samples directly quenched at 200 °C, 300 °C, and 400 °C.

nominal stoichiometry. When the nominal stoichiometry was $K_{0.8}Fe_2Se_2$, some groups saw clear superconductivity in the samples not quenched from high temperatures with the actual compositions as $K_{0.78}Fe_{1.70}Se_2$ [9] and $K_{0.80}Fe_{1.76}Se_2$ [13, 14] respectively. The iron valences of the two samples were also located at the non-superconducting region in the electronic and magnetic phase diagram. The phase diagram makers reported that their $K_{0.8}Fe_2Se_2$ sample was also superconducting and had an actual composition of $K_{0.73}Fe_{1.67}Se_2$. In sharp contrast to their results, we never see superconductivity in not quenched samples when the nominal composition is $K_{0.8}Fe_2Se_2$ as well and the actual composition is similar to one of the actual compositions reported by other groups, $K_{0.78}Fe_{1.70}Se_2$. In consideration of these different results, we think that the property of $K_xFe_{2-y}Se_2$ is sensitive to preparation conditions. Many conditions such as the quality of quartz tube and the warm-keeping performance of furnace all have influences on the property of $K_xFe_{2-y}Se_2$. For instance, the different actual compositions of $K_xFe_{2-y}Se_2$ among the samples prepared by different groups may be caused by the different qualities of quartz tubes which make different loss of K in amount. The different transport properties of $K_xFe_{2-y}Se_2$ even among the samples not quenched with similar actual compositions may be caused by the different warm-keeping performances of furnaces which make different cooling rates after the furnaces are turned off. We control the preparation conditions consistent, so our result is repeatable, credible and not contradictory to other different experimental results.

3.2. Post-annealing and then quenching

By post-annealing and then quenching at 200 °C, 300 °C, and 400 °C, we tune the No.1 sample from insulating to superconducting. In Fig.4 we show the temperate

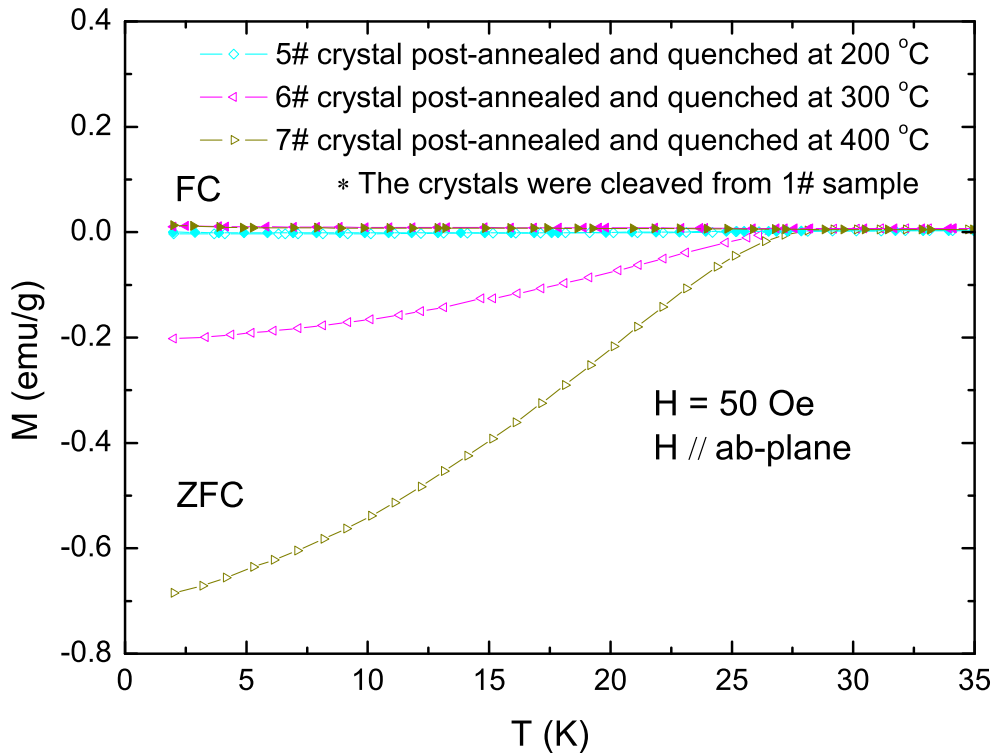


Figure 4. (Color online) Temperature dependence of dc magnetization for the crystals post-annealed and then quenched at at about 200 °C, 300 °C, and 400 °C, which were cleaved from No.1 sample in advance. The measurements were carried out under a magnetic field of 50 Oe in zero-field cooled (ZFC) and field-cooled (FC) processes with the field parallel to the ab-plane.

dependence of dc magnetization for the crystals post-annealed and then quenched at about 200 °C, 300 °C, and 400 °C, respectively. The measurements were carried out under a magnetic field of 50 Oe in zero-field-cooled (ZFC) and field-cooled (FC) processes with the field parallel to the ab-plane. There is not a diamagnetic signal observed in the crystal post-annealed and quenched at 200 °C. When the annealing and quenching temperature increases to above 300 °C, diamagnetic signals begin to appear below about 26 K. We find that the annealing and quenching temperature has an important influence on the diamagnetization signal like the condition of direct quenching. However, the diamagnetic signals of the crystals post-annealed and then quenched are not as strong as the ones of the samples directly quenched under the same quenching temperatures.

By electrical resistivity measurements we find that the post-annealed and quenched crystals' transport characters are getting different from the No.1 sample, as shown in Fig.5. The crystal after post-annealing and quenching at 200 °C has a semiconducting/insulating behavior from 30 to 300 K and the resistivity drops when the temperature decreases below 30 K. The dropping may imply that more metallic phase is achieved corresponding to the superconductivity. The crystal post-annealed and quenched at 300 °C has been tuned to superconducting state and there is a hump-like anomaly at 155 K in the curve of $\rho(T)$. The crystal post-annealed and quenched at 400 °C is also superconducting and the hump-like anomaly shifts to about 250 K. We also find that the absolute value of resistivity decreases with increasing the quenching temperature from 200 to 400 °C.

We also carried out X-ray diffraction on these crystals. As shown in Fig.6, the peaks from the (00 l) reflections are still very sharp after annealing. We still hardly find very obvious shifting among these peaks. And the peaks marked by the asterisks seem to shift closer to the nearby (008) and (00 $\bar{1}0$) peaks after annealing and

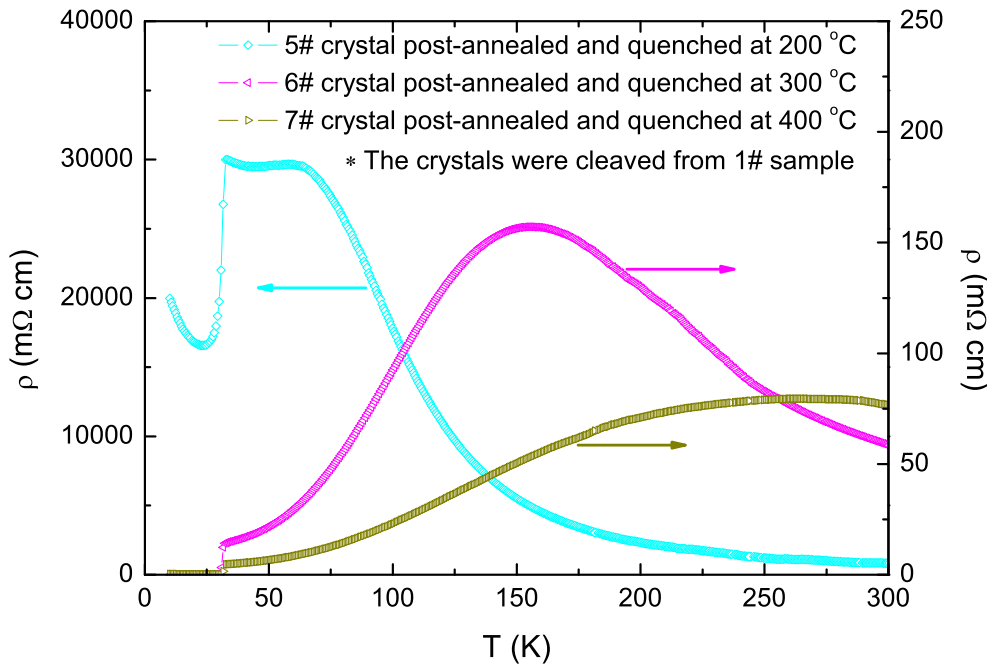


Figure 5. (Color online) Temperature dependence of resistivity for the crystals post-annealed and then quenched at at about 200 °C, 300 °C, and 400 °C, which were cleaved from No.1 sample in advance.

quenching. This feature is similar to the case of direct quenching.

Surprisingly, the crystals post-annealed and quenched lost their superconducting characters after a period of time, for example, 20 days later. In this period the crystals were always kept in the argon atmosphere. As shown in Fig.7, after 20 days, the strong diamagnetization signal has disappeared and the insulating state comes out again in the No.7 crystal. Obviously, the superconducting state tuned from the insulating state by post-annealing and quenching is unstable. However, there is no time dependence of superconductivity observed in our directly quenched samples and reported by other groups, which suggests that the freezing effect of post-annealing and quenching is temporary and less effective than directly quenching.

4. Conclusions

In summary, we find that the samples directly quenched in the cooling process of growth show superconducting while the one cooled with furnace is insulating, and the latter can be tuned from insulating to superconducting by post-annealing and then quenching. In addition, the actual compositions and the iron valences of all the non-superconducting and superconducting samples are very similar to each other since we fixed the nominal stoichiometries in preparing process. Based on the two factors, we conclude that the superconducting state in $K_xFe_{2-y}Se_2$ is metastable, and quenching is the key point to achieve the superconducting state. The similar stoichiometries of all the non-superconducting and superconducting samples also indicate that the iron valence doesn't play a decisive role in determining whether a $K_xFe_{2-y}Se_2$ sample is superconducting. Our result in resistivity indicates that $K_xFe_{2-y}Se_2$ is a phase-separation system composed of a metallic phase and a insulating phase. Our XRD results suggest that there is a super-lattice of iron vacancies order in this system and the phase with iron vacancies is less in the superconducting samples than in the insulating samples. All these results give a support to the Mössbauer result reported before that the superconductivity in $K_xFe_{2-y}Se_2$ comes from a minority phase which does not have large moment and the long range

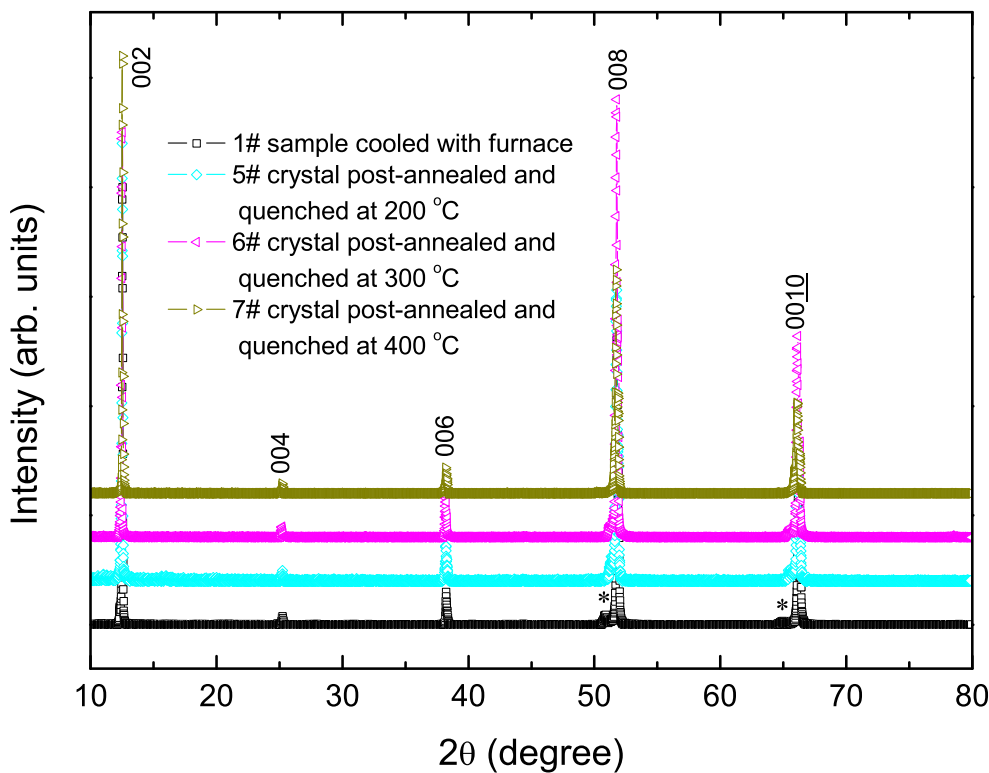


Figure 6. (Color online) X-ray diffraction patterns showing the $(00l)$ reflections from the basal plane of the $K_x\text{Fe}_{2-y}\text{Se}_2$ sample cooled with furnace and the crystals post-annealed and then quenched at about 200 °C, 300 °C, and 400 °C. The samples undergoing different treating processes were cleaved from the sample cooled with furnace and not superconducting.

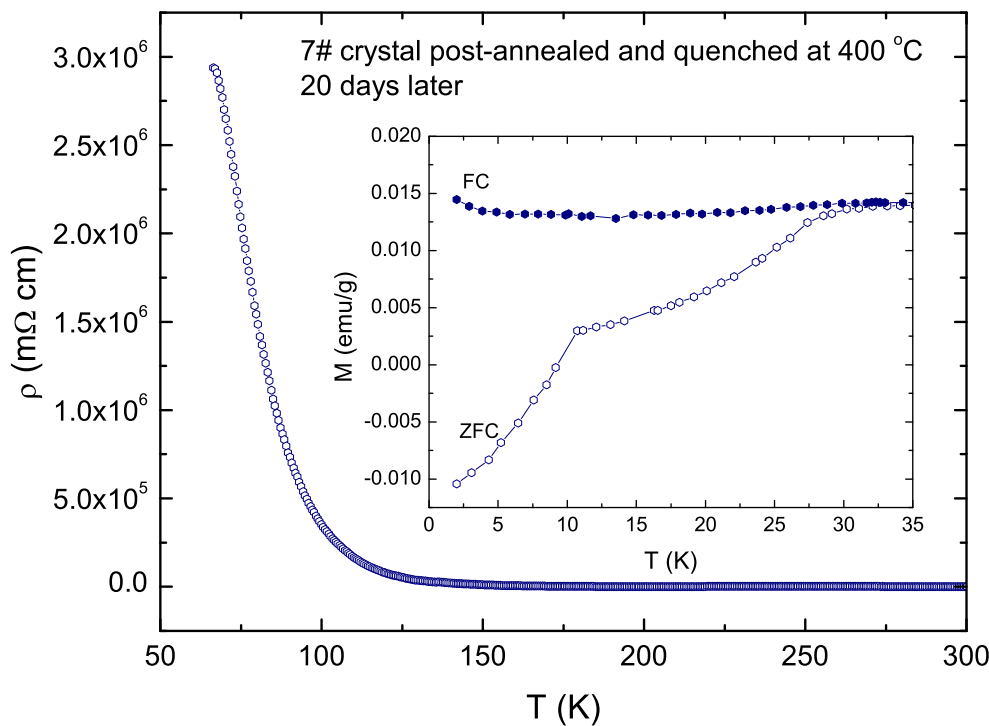


Figure 7. (Color online) After 20 days, the temperature dependence of dc magnetization and resistivity for the crystal post-annealed and quenched at 400 °C.

magnetic order belongs to a non-superconducting majority phase[16]. Combining with the result obtained in the $K_x\text{Fe}_{2-y}\text{Se}_2$ thin films prepared by molecular beam epitaxy (MBE)[17], we argue that our superconducting sample partly corresponds to the phase without iron vacancies as seen by scanning tunneling microscopy (STM), and the insulating sample mainly corresponds to the phase with $\sqrt{5} \times \sqrt{5}$ iron vacancy order. Quenching may play a role of freezing the phase without iron vacancies. Therefore, whether the $K_x\text{Fe}_{2-y}\text{Se}_2$ sample contains the phase without iron vacancies is more essential to achieve superconductivity, instead, the iron valence does not play an important role. By varying the ratio of starting materials to tune the iron valence or quenching a sample with fixed stoichiometry are both effective to obtain the superconducting state. There is, perhaps a difference, that the superconducting state tuned by varying the ratio of starting materials is more stable, while the superconducting state frozen by quenching is metastable.

Acknowledgements

This work is supported by the Natural Science Foundation of China, the Ministry of Science and Technology of China (973 project: 2011CBA00102).

References

- [1] Y. Kamihara, T. Watanabe, M. Hirano, and H. Hosono, *J. Am. Chem. Soc.* 130 (2008) p.3296.
- [2] M. Rotter, M. Tegel, and D. Johrendt, *Phys. Rev. Lett.* 101 (2008) p.107006.
- [3] K. Sasmal, B. Lv, B. Lorenz, A. Guloy, F. Chen, Y. Xue, and C. W. Chu, *Phys. Rev. Lett.* 101 (2008) p.107007.
- [4] X. C. Wang, Q. Q. Liu, Y. X. Lv, W. B. Gao, L. X. Yang, R. C. Yu, F. Y. Li, and C. Q. Jin, *Solid State Commun.* 148 (2008) p.538.
- [5] J. H. Tapp, Z. Tang, B. Lv, K. Sasmal, B. Lorenz, P. C. W. Chu, and A. M. Guloy, *Phys. Rev. B* 78 (2008) p.060505(R).
- [6] F. C. Hsu, J. Y. Luo, K. W. Yeh, T. K. Chen, T. W. Huang, P. M. Wu, Y. C. Lee, Y. L. Huang, Y. Y. Chu, D. C. Yan, and M. K. Wu, *Proc. Natl. Acad. Sci.* 105 (2008) p.14262.
- [7] T. Klimczuk, T.M. McQueen, A.J. Williams, Q. Huang, F. Ronning, E.D. Bauer, J.D. Thompson, M.A. Green, and R.J. Cava, *Phys. Rev. B* 79 (2009) p.012505.
- [8] X. Zhu, F. Han, G. Mu, P. Cheng, B. Shen, B. Zeng, and H. H. Wen, *Phys. Rev. B* 79 (2009) p.220512(R).
- [9] J. Guo, S. Jin, G. Wang, S. Wang, K. Zhu, T. Zhou, M. He and X. Chen, *Phys. Rev. B* 82 (2010) p.180520(R).
- [10] D. M. Wang, J. B. He, T. L. Xia, and G. F. Chen, *Phys. Rev. B* 83 (2011) p.132502.
- [11] M. H. Fang, H. D. Wang, C. H. Dong, Z. J. Li, C. M. Feng, J. Chen, and H. Q. Yuan, *Europhys. Lett.* 94 (2011) p.27009.
- [12] Y. J. Yan, M. Zhang, A. F. Wang, J. J. Ying, Z. Y. Li, W. Qin, X. G. Luo, J. Q. Li, J. Hu, and X. H. Chen, *arXiv:cond-mat/1104.4941* (2011).
- [13] R. Hu, K. Cho, H. Kim, H. Hodovanets, W. E. Straszheim, M. A. Tanatar, R. Prozorov, S. L. Bud'ko and P. C. Canfield, *Supercond. Sci. Technol.* 24 (2011) p.065006.
- [14] E. D. Mun, M. M. Altarawneh, C. H. Mielke, V. S. Zapf, R. Hu, S. L. Bud'ko, and P. C. Canfield, *Phys. Rev. B* 83 (2011) p.100514(R).
- [15] H. Lei, and C. Petrovic, *arXiv:cond-mat/1110.5316* (2011).
- [16] D. H. Ryan, W. N. Rowan-Weetaluktuk, J. M. Cadogan, R. Hu, W. E. Straszheim, S. L. Bud'ko, and P. C. Canfield, *Phys. Rev. B* 83 (2011) p.104526.
- [17] W. Li, H. Ding, P. Deng, K. Chang, C. Song, K. He, L. Wang, X. Ma, J. P. Hu, X. Chen, and Q. K. Xue, *Nat. Phys.* 8 (2012) p.126.